FORMATION ANALYSIS

Using wavelets to determine paper formation by light transmission image analysis

MOUADE BOUYDAIN, JOSE F. COLOM, AND JOSEP PLADELLORENS

ABSTRACT

Quantitative determination of paper formation has been a difficult problem to solve. This paper presents a method using light transmission image analysis with wavelets to decompose the image and analyze the floc distribution from the energy of the images resulting by the decomposition. Testing of the method for various furnishes indicates that it is more sensitive to different qualities of formation than the standard formation number.

Application:

A method using light transmission image analysis quantitatively determines the formation of paper.

THE INTERNATIONAL STANDARDS office defines formation as the distribution, disposition, and intermixing of fibers to constitute paper. The main goal of the papermaking process is to distribute these fibers as evenly as possible to provide uniformity. Factors that influence variations in local grammage relate to fiber characteristics *(1-4)*. They are generally small-scale variations due to natural fiber flocculations or flocculations induced by high frequency pulsations. Large-scale variations in the local grammage relate to instabilities of the manufacturing process *(5-9)*.

Although paper formation is important for those concerned with paper production, it has been a difficult property to determine. Fast, quantitative, and convenient methods could make automatic inspection of sheet formation possible. In this work, we try to develop a method using wavelet theory to find a new index of formation that is more sensitive to local grammage variations.

CHARACTERIZATION OF SHEET FORMATION AND FLOC STRUCTURE

Various formation indices provide quantitative definitions of paper formation. They are quantitative representations of local grammage, histograms, or maps of local grammage. All try to characterize accurately the distribution of the fibers in the sheet of paper under study.

The most common index is the standard deviation of local grammage in a small zone of the sheet divided by the mean value of local grammage in the entire sheet. This is the standard formation number (FN) *(1)*. It has some limitations because sheets with very different formation may have the same formation number. Other indices are available in the literature such as Dodson's formation number *(9)*. This compares an ideal formation sheet and a particular sheet. Another work by Jordan *(10)* defines flocs as regions of heavier than median grammage. His index is a threshold equal to the mean grammage. It calculates the ratio of the sum of floc perimeters for a sample to the size of the sample. The method is sensitive to paper structure and the graininess of the flocs.

Statistical analysis using the power and wavelength spectra *(1, 11)* provides a description of the different contributions to the variance in frequency intervals. Although the method relates directly to floc size, it only considers periodic variations and treats the paper as one-dimensional. This provides an incomplete description of floc structure since it gives no information on how basis weight variations distribute through the sample. For example, it cannot describe the coarseness of formation or the distribution of the size of the grammage and grammage intensity—paper quality.

Second order statistics *(11, 12)* treat paper as two-dimensional. They provide five indices dealing with the "co-occurrence matrix" by computing the probability of occurrence of some predefined matrices from the original image. These indices—frequency, distribution, and formation quality—indirectly relate to the floc size. They are therefore difficult to interpret.

Bernie *(13)* defined another index using fast Fourier transform treatment of the data extracted from a contour map of the flocs in paper. Using light transmission, this method examines a grid of pixels seen as a grammage matrix.

In this work, we used a wavelet decomposition of the image of paper obtained by light transmission in a light box. Wavelets gave a multiresolution analysis that was very appropriate for analysis of the flocculation of paper at different scales.

WAVELETS AND MULTIRESOLUTION

To analyze the image of the paper, we performed a multiresolution analysis *(14)*. This means that a given signal—two-dimensional—was decomposed at a coarse approximation plus added details. In other words, the detail signal was the difference between the coarse and fine versions of the signal. Applying the

Coefficient	Value of the coefficient
h (0)	0.054415842243
h (1)	0.312871590914
h (2)	0.675630736297
h (3)	0.585354683654
h (4)	-0.015829105256
h (5)	-0.284015542962
h (6)	0.000472484574
h (7)	0.128747426620
h (8)	-0.017369301002
h (9)	-0.044088253931
h (10)	0.013981027917
h (11)	0.008746094047
h (12)	-0.004870352993
h (13)	-0.000391740373
h (14)	0.000675449406
h (15)	-0.000117476784

I. The 16-tap Daubechies wavelet filter coefficients

successive approximations recursively makes the approximation error go to zero.

Using multiresolution analysis and orthonormal wavelet bases from Eq. 1 below, Mallat *(14)* constructed an algorithm using wavelet functions that is economical and powerful in its orientation selectivity. His decomposition provides one representation with one desired resolution version of the original image at some level, j, for example sampled twice as sparsely as its predecessor. He adds details corresponding to the difference in information between the resolution at level j and at level j – 1 separated into levels corresponding to different spatial frequency bands—horizontal high frequency band, vertical high frequency band, and diagonal high frequency band.

For a one-dimensional discrete signal,the following is a decomposition. From a data sequence C_0 with k entries, we construct the function f_0 (x) defined by:

$$f_0(x) = \sum_k c_{0,k}\phi_{0,k}(x) \qquad (1)$$

where

ϕ is a scaling function that satisfies a two-scale difference equation:

$$\phi(x) = (2)^{1/2}\sum_k h(k)\phi(2x - k) \qquad (2)$$

Such a decomposition provides a coarse approximation of the signal.

The details of the signal are obtained by a decomposition of such data sequences with a family of real orthonormal bases, $\psi_{j,k}(x)$, obtained through a translation and dilation of a function, ψ, known as a mother wavelet, i. e.,

$$\psi_{j,k}(x) = 2^{-j/2}\psi(2^{-j}x - k) \qquad (3)$$

where

j and k are integers.

The mother wavelet, $\psi(x)$, is constructed from a scaling function, $\phi(x)$, using the following:

$$\psi(x) = (2)^{1/2}\sum_k g(k)\phi(2x - k) \qquad (4)$$

where

$$g(k) = (-1)^k\, h(1-k) \qquad (5)$$

At some desired level, J, the function, f_0, can be written as:

$$f_0(x) = \sum_k c_{j+1,k}\phi_{j+1,k}(x) + \sum_{j=0}^{J} d_{j+1,k}\psi_{j+1,k}(x) \qquad (6)$$

where

$0 < j < J$.

The coefficients, $c_{j+1,n}$ and $d_{j+1,n}$, at scale, j + 1, relate to the coefficients, $c_{j,k}$, at scale, j, using the following:

$$c_{j+1,n} = \sum_k c_{j,k}h(k - 2n)$$

and

$$d_{j+1,n} = \sum_k c_{j,k}g(k - 2n) \qquad (7)$$

The decomposition is therefore a filtering of the data through two filters, H and G, with impulse response, $h^{\sim}(n)$ and $g^{\sim}(n)$. This gives a recursive algorithm for wavelet decomposition. We can also deduce the following:

$$c_{j,k} = \sum_k c_{j+1,n}h(k - 2n) + \sum_k d_{j+1,n}g(k - 2n) \qquad (8)$$

The filter coefficients, h(k) and g(k), constructed by Mallat from the multiresolution are sufficient. Explicit forms of $\phi(x)$ and $\psi(x)$ are not necessary to perform this wavelet decomposition.

Daubechies showed later that such filter coefficients, h(k), can be constructed without reference to the multiresolution analysis by imposing some conditions onto those filter coefficients to make the algorithm work (15). This also allows the set of basic wavelet functions expressed in Eq. 1 to be unique, orthonormal, and compact. They also have a certain degree of regularity so that the reconstruction of the image looks reasonably good even after several iterations. **Table I** gives the Daubechies filter coefficients.

The two dimensional wavelet basis functions can be expressed by the tensor product of two one-dimensional wavelet basis functions along the horizontal and vertical directions. The data sequences to be decomposed are now $C^0 = (C^0_{m,n})$ where m and n are integers. The corresponding two dimensional filter coefficients can be expressed as $H_c.H_r$, $G_c.H_r$, $H_c.G_r$, and $G_c.G_r$ with c and r indicating respective columns and rows. For example, the decomposition for one iteration of the data sequences $(C^0_{m,n})$ gives new data sequences C^1 and three different sequences (details): $d^{1,1}$, $d^{1,2}$, and $d^{1,3}$ as follows:

$$\begin{aligned} C^1 &= H_c.Hr\, C^0 \\ d^{1,1} &= G_c.H_r C^0 \\ d^{1,2} &= H_c.G_r C^0 \\ d^{1,3} &= G_c.G_r C^0. \end{aligned} \qquad (9)$$

The operator, $G_c.H_r$ smooths the column index and looks at the difference (high frequency information)

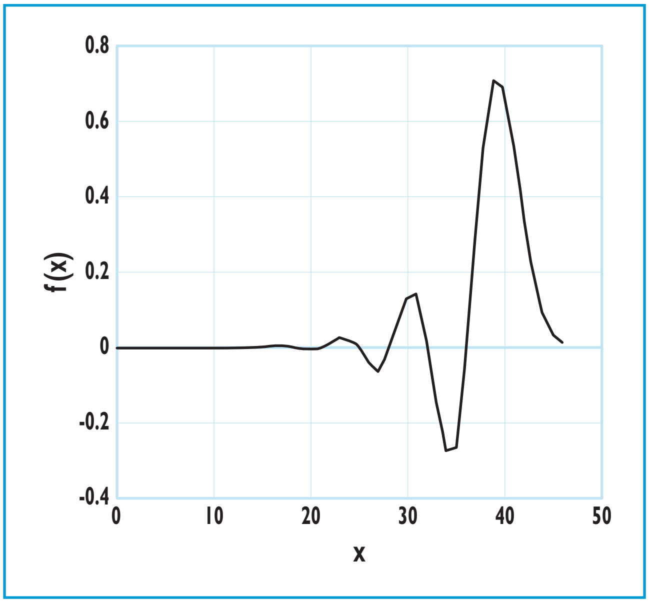

1. Scaling function related to the 16-tap Daubechies wavelet coefficients for two iterations

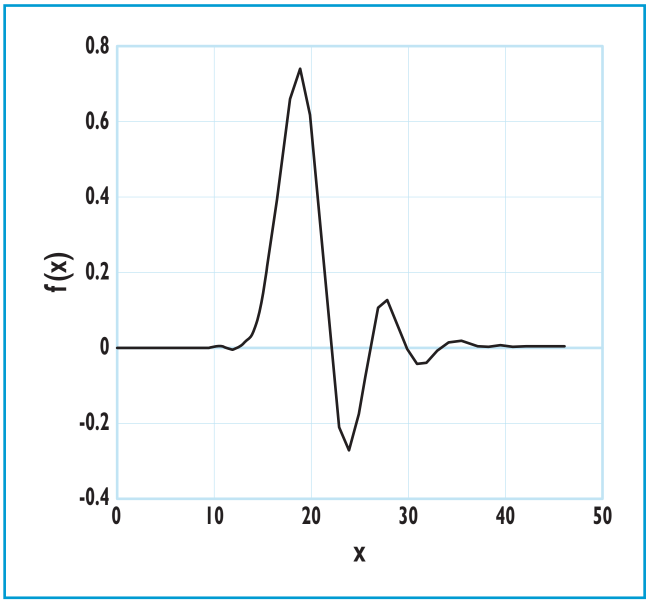

2. Wavelet function related to the 16-tap Daubechies wavelet coefficients for two iterations

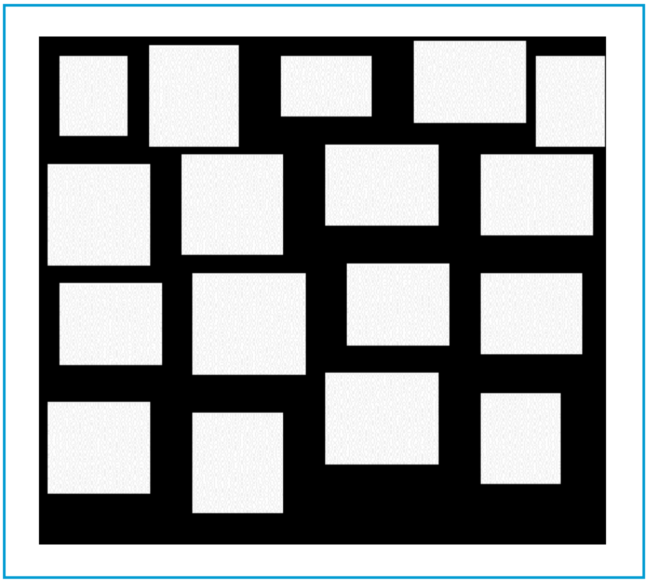

3. Simulated image 1 with small blocks

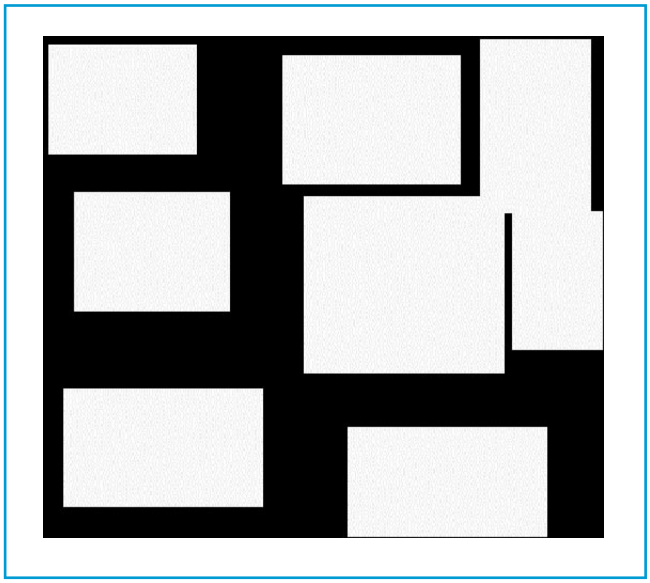

4. Simulated image 2 with large blocks

for the row index. Then, $d^{1,1}$ will be large when a horizontal edge is present. This shows clearly that the algorithm used in this work is orientation sensitive. **Figures 1 and 2** show the scaling and wavelet functions used in this work.

EXAMPLE

To clarify the procedure, we simulated two matrices using images of two papers with different formation quality. We applied the wavelet orthonormal basis of Daubechies with 16 coefficients to the same wavelet transform as the real images of the papers used in our work. This makes the effect of the method visual and numerical to characterize the different variations in each image accurately.

The blocks of image 1 in **Fig. 3** are smaller than those of image 2 in **Fig. 4**. This makes the first image have more variations than the second. The coefficients in the decomposition would therefore be higher in image 2 than in image 1. **Figures 5 and 6** show the decomposition images successively for the two matrices.

The sum of the energies in each band of the decomposition has the following definition:

$$\text{Sum of energies} = \sum_{a=1}^{3} E_a$$

$$\text{with } E_a = \sum_i \sum_j x_{ij}^2 \tag{10}$$

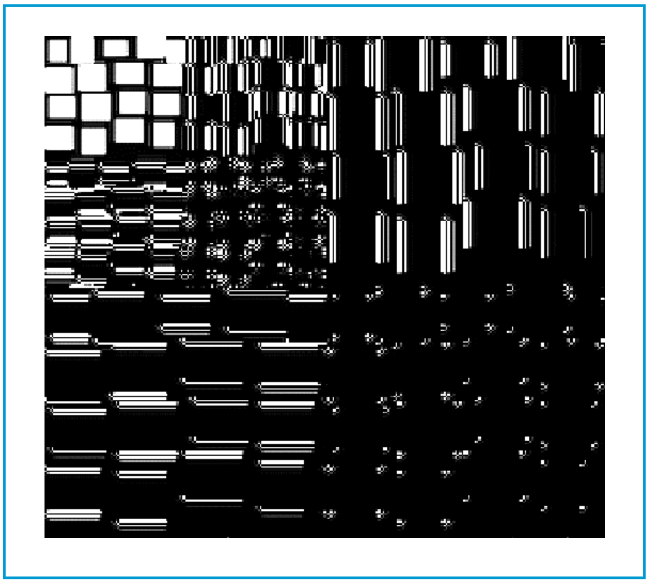

5. Wavelet decomposition representation for image 1

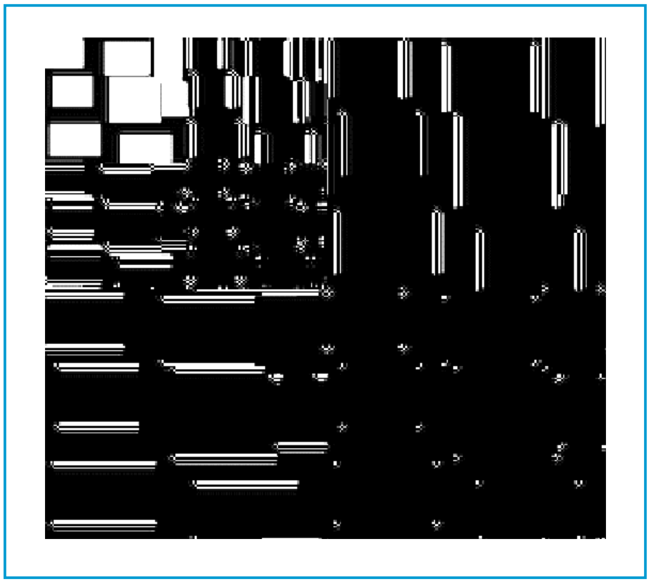

6. Wavelet decomposition representation for image 2

	Image 1	Image 2
Energy of Band 1	2.31×10^7	1.488×10^7
Energy of Band 2	2.03×10^7	1.802×10^7
Energy of Band 3	2.35×10^7	1.208×10^5

II. Values of energy in the bands of the second iteration of the decomposition of images 1 and 2

where

a = the band number, x_{ij}, a value of each pixel in the corresponding band.

Table II shows that the energy sum is higher for image1 than for image 2.

EQUIPMENT AND METHOD

Figure 7 shows the equipment used. A black and white camera acquired the image of a sheet of paper with size 6.2 cm x 6.3 cm placed on a light box and sent it to a computer via an acquisition card. Suitable software for processing produced an image on a 512 x 512 grid with 256 gray levels.

Since an image analysis system requires a large memory, we used equipment that had sufficient memory and hard drive and a high processing speed.

Because we made the images using light transmission with a light box, we had to remove the effect of nonuniform lighting produced by the light box after the acquisition of the image and the coding on 8 bits. The correction uses a pixel-to-pixel division between the image and the image of the light box. We then applied Daubechies' wavelet orthonormal basis with 16 coefficients to decompose the image of each paper under study.

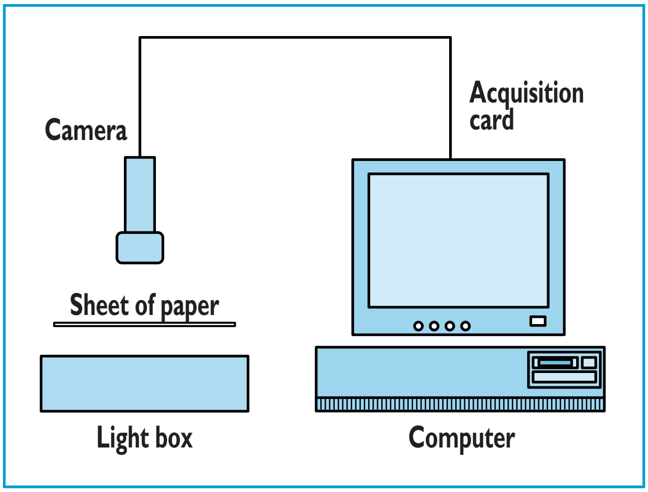

7. Equipment for this work

APPLICATION WITH PAPER

Figures 8–10 show images of three sheets of paper with different fiber natures. They therefore have different quality formations that correspond respectively to papers manufactured with short fibers of softwood (FIBC), long fibers of hardwood (FIBL), and equal mixtures of short and long fibers (FIBCL). Tests used handsheets of 60 g/m².

The images were obtained with the equipment shown in Fig. 7 using the same optical conditions for all images. We first normalized the images obtained from the sheets so they all had the same energy before processing. Then we applied Daubechies' wavelet transform to decompose those matrices or images into a low frequency band (band 0) and high frequency bands (band 1, band 2, and band 3). This separated the details caused by changes in local grammage in different directions:

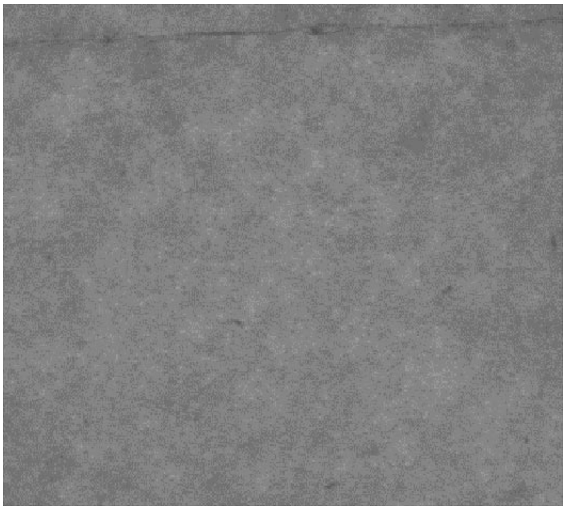

8. Light transmission image for FIBC

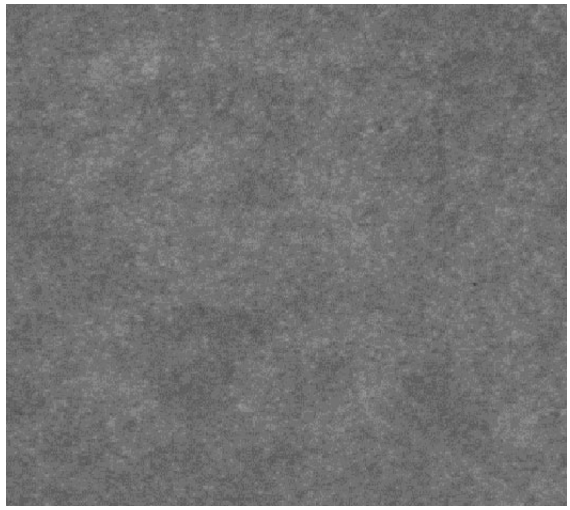

9. Light transmission image for FIBCL

Band 0: Approximation of the image at coarse resolution
Band 1: Horizontal changes
Band 2: Vertical changes
Band 3: Diagonal changes.

We applied the transform twice—two iterations—for each matrix because a difference in formation is present in the middle frequencies. The corresponding bands for which we calculated the energy represent all information between the first and the second approximation:

Band 2-0: Residue of the image after decomposition
Band 2-1: Complete horizontal changes between the first and second approximation
Band 2-2: Complete vertical changes between the first and second approximation
Band 2-3: Complete diagonal changes between the first and second approximation.

The wavelet formation index, WI, is the sum of energies of the particular bands—middle frequency bands. It provides information for the flocs only and not for the small scale changes or low frequency bands. The low frequency bands result from the following:

$$WI = \sum_{a=1}^{3} F_i \text{ with } F_i = \sum_i \sum_j x_{ij}^2 \qquad (11)$$

where
a = the band number
x_{ij} = the value of each pixel in the corresponding band.

We also calculated the standard formation number of each of the sheets of paper to compare with the wavelet formation index and justify the validity of the method.

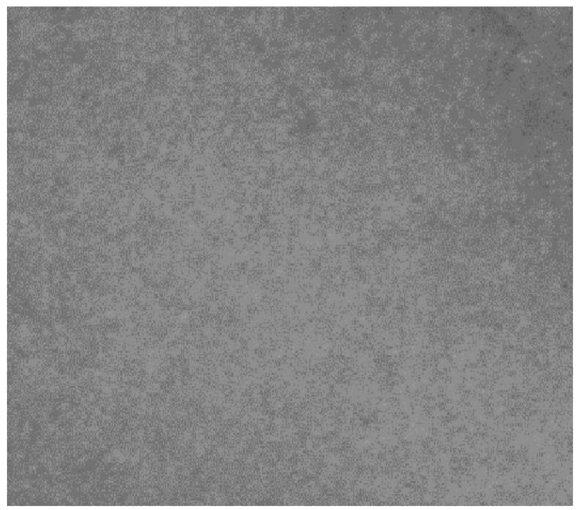

10. Light transmission image for FIBL

The standard formation number comes from the following:

$$FN(A) = \sigma(w_A)/w_M \text{ with } \sigma^2 = \sum_i \sum_j (x_{ij} - x_m)^2 \qquad (12)$$

where

$\sigma(w_A)$ = the standard deviation of the values of the pixels in the zone W_A
w_A = the studied zone of the image
x_M = the mean value in the zone w_A
w_M = the mean value in the total image.

With this processing, one would expect a sheet with uniform local grammage to have a WI value of zero. The poor

	FIBC	FIBL	FIBCL
FN	0.038	0.048	0.041
Energy of band 2-1	3.06×10^5	1.46×10^6	6.24×10^5
Energy of band 2-2	4.38×10^5	2.06×10^6	9.56×10^5
Energy of band 2-3	1.24×10^5	4.88×10^5	2.29×10^5
WI	8.68	40.08	18.09

III. Values of the standard FN, energies in the bands, and WI for FIBC, FIBL, and FIBCL

	FIBC/FIBL	FIBL/FIBCL	FIBCL/FIBC
FN	1.26	1.17	1.08
WI	4.26	2.21	2.08

IV. Comparative values of standard FN and WI for the three sheets of papers

formation would have higher WI. **Table III** gives results for application of the method to the sheets of paper cited above. **Table IV** compares the two formation indices for FIBL and FIBC. WI is 326% higher, but the standard formation number is 26% higher. A comparison between FIBL and FIBCL shows that WI is more sensitive than the standard formation number.

SUMMARY

We have developed a quantitative method to determine the formation of paper. The method is based on light transmission image analysis. It uses wavelets to decompose the image and analyze the floc distribution from the energy of the images resulting from the decomposition. We analyzed the image of paper performing a multiresolution analysis. This means that a given signal—a two-dimensional signal in our case—was decomposed at a coarse approximation plus added details. The detail signal is the difference between the coarse and fine versions of the signal. By applying successive approximations recursively, the approximation error goes to zero. Flocculations in a paper may be considered "details." Measuring the energy associated with these details determines the formation of a paper. Before application to paper, we used the method as an example on two computer-created images. This showed the behavior of the energy of the decomposition with respect to the variations inside the images.

The method was tested with various formations and compared with the standard formation index. The new technique discriminates more sensitively between different qualities of formation than the standard formation number. **TJ**

Bouydain and Pladellorens are Ph.D. student and professor, respectively, at Department of Optics and Optometry, Universitat Politecnica de Catalunya, Violinista Vellsola 37, 08222 Terrassa, Spain, and Colom is professor at Departament of Textile and Paper Engineering, Universitat Politecnica de Catalunya, Colom 10, 08222 Terrassa, Spain.

Received for review Feb. 9, 1998.
Accepted June 29, 1998.

Acknowledgments: Comision Interministerial para la ciencia y la Tecnologia (CICYT) financed this work under grant number TAP 97-1089.

LITERATURE CITED

1. Sara, H., "*The characterization and measurement of paper formation with standard deviation and power spectrum*," Ph.D. thesis, University of Helsinki, Helsinki, Finland, 1978.
2. Herdman, P. T. and Corte, H., *Pulp Paper Can.* 81(10):81(1980).
3. Parker, I. H., *APPITA* 28(6):409(1975).
4. Corte, H. and Dodson, C. T. J., *Das Papier* 23:381(1969).
5. Perrault, J., *Pulp Paper Can.* 83(6):69(1982).
6. Cuthall, K. A. and Mardon, J., *APPITA* 28(4):252(1975).
7. Trepanier, R. J., Hodgson, P.W., and Quellette, R. J., *1985 Pulp and Paper Technology Conference*, Japan TAPPI and CPPA, Tokyo, p. 191.
8. Bergh, P. A., "*The application of image analysis to evaluate the structure and properties of paper*," Ph.D. thesis, State University of New York, Syracuse, NY, 1981.
9. Dodson, C. T. J., *Tappi J.* 76(5):153(1993).
10. Jordan, B. D. and Nguyen, N. G., "*Specific perimeter—a graininess parameter for formation and print-mottle textures*," Paprican, Vancouver, 1984, p. 484.
11. Cresson, T. and Luner, P., *Tappi J.* 73(12):175(1990).
12. Cresson, T. and Luner, P., *Tappi J.* 74(2):167(1991).
13. Bernie, J. P and Murray D. W. J., *Tappi J.* 79(1):193(1996).
14. Mallat, S. G, *IEEE Trans. Pattern Anal. and Machine Intell.* 11(7):674(1989).
15. Daubechies. I, *Communications on Pure and Applied Mathematics* 41(10):909(1988).